

# Multi-zone buildings thermo-hygrometric analysis: a novel dynamic simulation code based on adaptive control

**Annamaria Buonomano – Department of Industrial Engineering, University of Naples Federico II, Italy – [annamaria.buonomano@unina.it](mailto:annamaria.buonomano@unina.it)**

**Umberto Montanaro – Department of Industrial Engineering, University of Naples Federico II, Italy – [umberto.montanaro@unina.it](mailto:umberto.montanaro@unina.it)**

**Adolfo Palombo – Department of Industrial Engineering, University of Naples Federico II, Italy – [adolfo.palombo@unina.it](mailto:adolfo.palombo@unina.it)**

**Stefania Santini – Department of Electrical Engineering and Information Technology, University of Naples Federico II, Italy – [stefania.santini@unina.it](mailto:stefania.santini@unina.it)**

## Abstract

This paper presents a novel dynamic simulation model for the analysis of multi-zone buildings' thermal response and the assessment of building energy performance and indoor comfort. In this new release of the code, called DETECt 2.3, two important innovations are implemented. They regard the simulation model of multi-zone buildings, consisting of thermal zones totally enclosed in others, and the design of a novel temperature-humidity control algorithm. The developed innovative control strategy is based on a reference adaptive control scheme for the online adaptation of the control gains, with the aim of overcoming the well-known problems of classical fixed gain control algorithms. This feature will be a key tool for the next generation of building performance simulation codes (also toward NZEB analyses). Both the innovations embedded in the code can be exploited to simulate special indoor environments of hospitals / laboratories, rooms or museum halls. With the aim of showing the features and the potentialities of the simulation code coupled with the new control scheme, a suitable case study related to an expo indoor space of a museum building, including a display case with an accurate climate control, was developed. Details about heating and cooling demands and loads are provided. Good tracking performance for both the temperature and humidity control are obtained through the presented control scheme.

## 1. Introduction

A crucial challenge for the next generation of buildings is the capability to overcome the trade-off between low energy demands and high thermal and hygrometric comfort levels. The growing attention to these issues has led the research interest toward the use of building management strategies with the aim of improving both building energy efficiency and occupants' comfort. In this regard, Building Energy Performance Simulation (BEPS) tools play a key role. In the last years, recent advances in the numerical analysis based on computational methods, as well as computer calculation power, provided significant opportunities for developing and/or improving a new generation of BEPS codes. Here, particular attention was paid to: i) investigating new building envelope technologies and innovative HVAC systems, often supported by renewable energies; ii) implementing advanced control algorithms and systems (Shaikh P. H. et al. 2014).

The presented paper focuses on this specific framework. In particular, the article describes the new features included in DETECt 2.3, which updates a previous release (DETEct 2.2 (Buonomano A. and Palombo A. 2014)) validated by means of the BESTEST procedure. Specifically, DETECt 2.3 enables the simulation of multi-thermal zones (in particular of zones totally enclosed in others). Furthermore, it implements advanced thermo-hygrometric control actions able

to automatically adapt to the variations of the simulated system and its surrounding environment. The code, purposely developed by the authors for research aims, is conceived as a reliable thermo-hygrometric calculation tool for building energy design and performance analysis. DETECt allows one to dynamically calculate heating and cooling demands of multi-zone buildings and to assess the benefits of different and advanced building envelope techniques (PCM, BIPV, BIPV/T, sunspace, etc.). Thus, designs of high-performance buildings can be obtained. It is worth noting that often several research topics cannot be analysed by commercial BEPS codes (e.g. recent prototypal technologies, non-standard operating conditions, particular system scheduling, etc.). Such inconvenience can be exceeded by developing in-house codes such as DETECt. Here, updating and modifications of the included models can be carried out by authors for all the occurring research needs.

The aim of this paper is to show the effectiveness of the code in predicting the behaviour of building thermal zones with rigid thermo-hygrometric constraints. Such a goal is achieved by exploiting the features of the adaptive control scheme embedded into in DETECt 2.3, based on a new optimal model reference scheme (named LQ-EMRAC, Linear Quadratic Extended Model Reference Adaptive Control). The major advantage of this control technique is the control of the thermo-hygrometric variables for indoor spaces in uncertain conditions, without requiring an *a priori* knowledge of the building dynamics. To this aim, different from standard fixed gains techniques such as, for example, the PI approach implemented in the previous DETECt 2.2 release, the implemented control algorithm is able on-line to automatically vary its gains values to contract abrupt and unknown changes in the building behaviour and/or its features and external conditions. The idea behind this approach is to achieve great control flexibility and robustness in order to guarantee, at the same time, optimality with respect to a certain cost function subject to some constraints. The LQ-EMRAC approach extends and fuses the classical Model Reference Adaptive Control (MRAC) scheme that has been

proved to be effective in controlling uncertain plants (Di Bernardo M. et al. 2008), with an LQ algorithm, typical in the optimal control theory.

A suitable case study is here developed in order to show the effectiveness of the adopted approach. In particular, it refers to an indoor hall of a museum building with an included glass display case. Here, an accurate climate control (rigid constraints of temperature and humidity of the case indoor air) is required. As is well known, such an occurrence is mandatory in case of particular exhibited items contained in museum glass cases (e.g. archival artifacts, paper-based objects, etc.). Here, preservation techniques must be emphasized in order to avoid any irreversible damage. The case study building is located in the Mediterranean weather zone of Naples, southern Italy. To the best of the authors' knowledge, this is the first attempt in literature to model in BEPS codes: i) control by means of advanced schemes (able to guarantee rigorous constraints of temperatures and humidity, simultaneously); ii) thermal zones totally included into others.

## 2. Thermodynamic model

In this paper, a suitable resistive-capacitive (RC) thermal network simulation model (assuming 1D transient heat transfer) for the thermo hygrometric analysis of two thermal zones (one optionally completely enclosed in the other one) is described. It is embedded in the new release of DETECt (Buonomano A. and Palombo A. 2014). Through such a model, the assessment of the dynamics of temperatures and humidity, as well as of heating and cooling loads and demands, can be carried out. A sketch of the modelled RC thermal network is shown in Fig. 3. The calculation procedure concerns the heat flows between: i) the outdoor environment and the main modelled thermal zone (zone 1 in Fig. 3); ii) the zone 1 and the related included thermal zone 2 (Fig. 3). The following model simplifications are considered: i) the indoor air of each thermal zone is uniform and modelled as a single indoor air temperature node; ii) the building envelope of zone 1 is subdivided into  $M$  multi-layer elements (adopting a high order RC thermal network); iii) the

construction envelope of zone 2 is lumped in a single node; iv) each  $m$ -th multi-layer building element of zone 1 is subdivided in  $N$  sub-layers (of different thicknesses), where thermal masses and conductivities are uniformly discretised; v)  $N+2$  capacitive and surface nodes are accounted for each  $m$ -th envelope component of zone 1, while 1 node is referred to its indoor air; vi) 2 nodes are modelled for zone 2, each one for the lumped envelope and the indoor air.

For zone 1, in each  $\tau$ -th time step and for each  $n$ -th capacitive node ( $j = 1, \dots, N$ ) of the  $m$ -th element ( $m = 1, \dots, M$ ), the differential equation describing the energy rate of change of each temperature node of the building envelope is:

$$C_{m,n} \frac{dT_{m,n}}{dt} = \sum_{j=n-1}^{n+1} \frac{T_{m,j} - T_{m,n}}{R_{m,j}^{eq}} \quad (1)$$

where  $C$  and  $T$  are the thermal capacitance and temperature of the node, respectively.  $R_{m,j}^{eq}$  is the sum of the halves sub-layers thermal resistances  $R_{m,j}^{cond}$  (that links the  $n$ -th node to their neighbours, Fig. 3). For non-capacitive outer ( $n = 0$ ) and inner ( $n = N+1$ ) surface boundary nodes, the algebraic equation describing the heat transfer is:

$$\sum_{j=n-1}^{n+1} \frac{T_{m,j} - T_{m,n}}{R_{m,j}^{cv}} + \dot{Q}_{m,n} = 0 \quad (2)$$

$R_{m,j}^{cv}$  is either a convective (external  $R_{m,0}^{conv}$  or internal  $R_{m,N+1}^{conv}$ ) or a conductive resistance ( $R_{m,n}^{cond}$ ), depending on the side layer of the considered node (Fig. 3).  $R_{m,0}^{conv}$  and  $R_{m,N+1}^{conv}$  connect non capacitive nodes to those related to the outdoor air temperature ( $T_{out}$ ) and to the indoor air one ( $T_{in,1}$ ), respectively. In case of floor elements,  $T_{out}$  and  $R_{m,j}^{cv}$  are replaced with the ground temperature ( $T_{gr}$ ) and an equivalent thermal conductive resistance ( $R_{gr}^k$ ). The modelled forcing function  $\dot{Q}_{m,n}$  includes the incident solar and the long-wave radiation exchange acting on outer and inner surfaces of zone 1 (Buonomano A. and Palombo A. 2014).

A simplified approach is adopted for zone 2. Here, the differential equation describing the energy rate of change of the temperature node of the zone 2 envelope ( $T_{w,2}$ ) is calculated as:

$$C_{w,2} \frac{dT_{w,2}}{dt} = \sum_{j=1}^2 \frac{T_{in,j} - T_{w,2}}{R_j^{glob}} \quad (3)$$

where  $C_{w,2}$  is the envelope lumped thermal capacitance, whose indoor air temperature is  $T_{in,2}$ ;  $R_j^{glob}$  is a global thermal resistance that takes into account all the heat transfer effects. For zone 1,  $R_1^{glob}$  is calculated by adding the half sub-layer conductive thermal resistance of the zone 2 envelope node to the equivalent convective and radiative thermal resistance (modelled by a combined linearized convective-radiative thermal resistance). A simplified approach is considered for zone 2. Here, the radiative exchange only takes into account the long-wave fraction vs. the zone 1. Thus, for zone 2, the equivalent global thermal resistance ( $R_2^{glob}$ ) includes combined conduction and convection phenomena only.

The differential equations on the thermal network nodes related to the indoor air of zone 1 and zone 2 must be solved simultaneously with the system of eqs. (1), (2) and (3). The sensible energy rate of change of zone 1 and zone 2 indoor air masses (at  $T_{in,1}$  and  $T_{in,2}$ , respectively) can be calculated as:

$$C_{in,1} \frac{dT_{in,1}}{dt} = \sum_{m=1}^M \frac{T_{m,N} - T_{in,1}}{R_{m,N}^{conv}} + \frac{T_{w,2} - T_{in,1}}{R_1^{glob}} + \frac{(T_{out} - T_{in,1})}{R_v} + \frac{(T_{in,2} - T_{in,1})}{R_{v,zns}} + \dot{Q}_{g,1} \pm \dot{Q}_{AC,1} \quad (4)$$

$$C_{in,2} \frac{dT_{in,2}}{dt} = \frac{T_{w,2} - T_{in,2}}{R_2^{glob}} + \frac{(T_{in,1} - T_{in,2})}{R_{v,zns}} + \dot{Q}_{g,2} \pm \dot{Q}_{AC,2} \quad (5)$$

where the thermal resistances  $R_v$  and  $R_{v,zns}$  describe the air ventilation and infiltration thermal loads:  $R_v$  links the indoor air node of zone 1 to the external one (outdoor air at  $T_{out}$ ),  $R_{v,zns}$  links the indoor air node of zone 2 to the one related to zone 1.

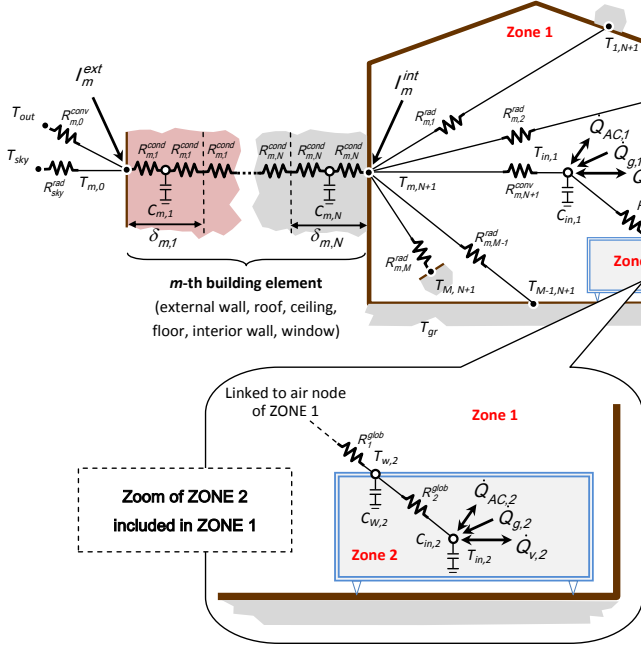


Fig. 3 – Sketch of the RC thermal network

Except for the thermal load due to the solar radiation transmitted through the windows and incident on the indoor surfaces, included in  $\dot{Q}_{m,n}$ , ( $I_m^{int}$ , Fig. 3), all the remaining sensible heat gains are considered as convective lumped heat source terms, networked to the indoor air nodes. They include: i) the thermal zone internal gains due to occupants, lights and equipment,  $\dot{Q}_{g,1}$  and  $\dot{Q}_{g,2}$ ; ii) the sensible heat to be supplied to (or removed from) the building space by an ideal HVAC system, aiming at maintaining the indoor air at the desired set point temperature,  $\dot{Q}_{AC,1}$  and  $\dot{Q}_{AC,2}$ . Therefore, the whole system including zone 1 and zone 2 is modelled through a thermal network of  $(M \times N) + 5$  nodes. The differential and algebraic equations describing the system thermal behaviour are: (1), (2), (3), (4) and (5).

The assessment of the latent energy to be added to (or subtracted from) both the thermal zones 1 and 2 (for maintaining the selected relative humidity set-point of the indoor air) is carried out by adopting a decoupled approach (Ghiaus C. 2014). For each indoor space the moisture balance is calculated by neglecting the moisture exchange between the air node and the surrounding building surfaces. In each  $\tau$ -th simulation time step and for each thermal zone ( $z = 1, 2$ ), the adopted moisture balance is:

$$\Omega_{in,z} \frac{d\omega_{in,z}}{dt} = \dot{m}_{v,z} (\omega_{out^*,z} - \omega_{in,z}) + \dot{m}_{wg,z} \pm \frac{\dot{Q}_{AC,z}^{lat}}{\Delta h_{vs}} \quad (6)$$

where  $\Omega_{in}$  is the indoor dry air mass;  $\dot{m}_v$  is the air ventilation mass flow rate;  $\dot{m}_{wg}$  is the inlet water vapour mass flow rate to the thermal zone (due to occupants);  $\omega_{out^*}$  and  $\omega_{in}$  are the external and indoor air specific humidity, respectively (note that the external air specific humidity is referred to: i) outdoor air for zone 1; ii) zone 1 air for zone 2);  $h_{vs}$  is the water latent evaporation heat at 0°C.

## 2.1 Reduced order model

For control aims, a linear simplified model was derived. Such a model stems from the above presented high order one (of  $(M \times N) + 2$  nodes (eqs. (1) and (2)) related to zone 1) which has been simplified into a linear and second-order model, exploited for the reference model design, where: i) the thermal capacity of the whole building envelope of zone 1 is lumped in a single node; ii) the input signals acting on the thermal network nodes are:  $T_{out}$ ,  $I^{ext}$ ,  $T_{gr}$  and  $\dot{Q}_{g,1}$ ; iii) an equivalent thermal resistance of the building envelope for internal and external surfaces is adopted; iv) weighted average thermal properties are assumed. Thus, eqs. (1) and (2) become:

$$C_{w,1} \frac{dT_{w,1}}{dt} = \frac{T_{out} - T_{w,1}}{R_{ext}^{eq}} + \frac{I^{ext} h_{out}^{eq}}{R_{ext}^{eq}} + \frac{T_{in,1} - T_{w,1}}{R_{int}^{eq}} + \frac{T_{gr} - T_{w,1}}{R_{gr}^{eq}} \quad (7)$$

As a consequence, equation (4) becomes:

$$C_{in,1} \frac{dT_{in,1}}{dt} = \frac{T_{w,1} - T_{in,1}}{R_{int}^{eq}} + \frac{T_{w,2} - T_{in,1}}{R_{int}^{glob}} + \frac{(T_{out} - T_{in,1})}{R_v} + \frac{(T_{in,2} - T_{in,1})}{R_{v,2ns}} + \dot{Q}_{g,1} \pm \dot{Q}_{AC,1} \quad (8)$$

As an example, for the sensible load calculation, the following vectors and matrices are considered: i) temperatures vector of the lumped envelope and indoor air thermal capacitances of both the zones,  $x_0 = [T_{w,1} \ T_{in,1} \ T_{w,2} \ T_{in,2}]$ ; ii) vector of sensible heat to be supplied or removed from the building space,  $u = [\dot{Q}_{AC,1} \ 0 \ \dot{Q}_{AC,2}]$ ; iii) the tuple  $(A_0, B_0, C_0)$  of dynamic matrix  $A_0$ , input and the output vectors  $B_0$  and  $C_0$  (e.g.  $B_0 = [0 \ C_{in,1}^{-1} \ 0 \ C_{in,2}^{-1}]^T$  and  $C_0 = [0 \ 1 \ 0 \ 1]$  for the sensible load calculation), see Section 3.

### 3. The enhanced optimal LQ-MRAC algorithm

In order to control the thermo-hygrometric behaviour, a new control scheme that enhances the classical Model Reference Adaptive Control (MRAC) strategy proposed by Landau (Landau I. D. (1979)) is adopted. The novel control algorithm (named Liner-Quadratic Enhanced Model Reference Adaptive Control, LQ-EMRAC) includes additional control actions to improve the closed-loop performance with respect to those provided by the more classical MRAC approach. Furthermore, it embeds as a reference model a rough plant model controlled via an LQ strategy (Anderson B.D.O. and Moore J.B. 1971). This implies that closed-loop dynamics, optimal with respect to a given performance index, are imposed to the plant under investigation via the adaptive action. More precisely, the reference model is a rough estimation of plant dynamics:

$$\dot{x}_0 = A_0 x_0 + B_0 u, \quad y = C_0 x_0 \quad (9)$$

(where  $x_0 \in \mathfrak{R}^n$  is the plant state,  $u, y \in \mathfrak{R}$  are the control input and the system output, respectively,  $A_0 \in \mathfrak{R}^{n \times n}$  is the dynamic matrix, and  $B_0 \in \mathfrak{R}^n$ ,  $C_0 \in \mathfrak{R}^{1 \times n}$  are the input and the output matrices, respectively, with  $n$  being the state space dimension) driven by a full state optimal feedback control action as:

$$u_{opt} = K^{opt} x_0 + K_R^{opt} r \quad (10)$$

being  $K^{opt} \in \mathfrak{R}^{1 \times n}$ ,  $K_R^{opt} \in \mathfrak{R}$  some fixed control parameters. From Optimal Control theory, it follows that the control signal in (10) minimizes a quadratic functional of the form:

$$J = \int_{t_0}^{+\infty} \left[ (y(t) - r)^T Q (y(t) - r) + u^T(t) R u(t) \right] dt \quad (11)$$

(where  $r \in \mathfrak{R}$  is the set-point to impose to the plant output,  $t_0$  is the initial time instant,  $Q \in \mathfrak{R}$  and  $R \in \mathfrak{R}$  are some positive matrices). As a result, the closed-loop optimal dynamics to be imposed to the plant are the solutions,  $x_m$ , of the following optimally-controlled time-invariant system:

$$\dot{x}_m = A_m x_m + B_m r \quad (12)$$

being  $A_m = A_0 + B_0 K^{opt}$  and  $B_m = B_0 K_R^{opt}$ . Details on the control algorithm and the control gains adaptation mechanism can be found in the following Appendix.

### 4. Case study and design of the LQ-EMRAC algorithm

The presented case study refers to a museum indoor space in which two thermal zones are modelled. In particular, the first zone refers to a museum hall while the second one (totally included in the first zone) to a glass display case with an accurate climate control (rigid constraints of temperature and humidity of the case indoor air) necessary to preserve collected exhibits such as: paints, woods, papers and leathers (which require suitable conditions of indoor air temperature and relative humidity, simultaneously). The sketch of the two-zone building is shown in Fig. 3. The simulation, carried out by DETECT 2.3, refers to the weather zone of Naples (southern Italy), by using a Meteororm hourly data file.

For zone 1, a typical Italian building envelope is taken into account, with length, width and height equal to 20, 10 and 3.5 m, respectively. The building's longitudinal axis is east-west oriented and a south-facing windows (4-6-4 air filled double-glazed system) of 32 m<sup>2</sup> is taken into account. The thickness of the building's walls and floor/ceiling are 25 and 30 cm, respectively. Their stratigraphy is designed by concrete bricks ( $\lambda = 0.51$  W/mK,  $\rho = 1400$  kg/m<sup>3</sup>,  $c = 1000$  J/kgK) and thermal insulation ( $\lambda = 0.04$  W/mK,  $\rho = 15.0$  kg/m<sup>3</sup>,  $c = 1400$  J/kgK). Note that each building element is subdivided in 10 sub layers of equal thickness. The direct solar radiation transferred through the windows to the inside zone is assumed to be absorbed by the floor with an absorption factor of 0.3. The absorption and emission factors of interior surfaces are assumed to be equal to 0.15 and 0.9, respectively. For such a zone, a ventilation rate equal to 1 Vol/h and a crowding index of 0.12 person/m<sup>2</sup> are taken into account. A cubic shaped zone 2 with a 1 m length side is considered. In particular, a glass envelope of 3 cm thickness, with an occurring air infiltration of 2 l/h is modelled.

The simulation starts on 0:00 of January 1<sup>st</sup> and ends at 24:00 of December 31<sup>st</sup>. The heating/cooling system of the thermal zone 1 is switched on from 07:00 to 18:00, from November 1<sup>st</sup> to March 31<sup>st</sup> (heating mode) and from June 1<sup>st</sup> to September 30<sup>th</sup> (cooling mode). The heating and cooling set points

indoor air temperature are set at 19 and 25°C, respectively. The relative humidity of the zone 1 indoor air is controlled at 50%. The heating/cooling system of the thermal zone 2 is switched on 24/7 to accurately conserve the case exhibited items. Here, the indoor air temperature and relative humidity are controlled throughout the year at 20°C and 65%, respectively.

The LQ-EMRAC has been implemented to control the air temperature and humidity, simultaneously, of both the modelled thermal zones. In particular, following a decentralized control approach (each control variable is used to impose the dynamic behaviour of only one variable to be controlled, see Pedro A. and Sala A. (2004)), four different and independent adaptive controllers are synthesized. In order to design the LQ-EMRAC control, the simplified models (see Section 2.1) were adopted as nominal models to be optimized via the LQ approach, by setting to zero the disturbance acting on the plant dynamics. Note that the choice of these simplified models reduces the complexity of the control design, without jeopardizing the closed-loop performance. Note that the optimality and robustness of the closed-loop control is guaranteed by the adaptive actions, whose gains evolve to compensate any parameter mismatch and/or presence of unmodelled dynamics (see Appendix), and to assure the minimization of a quadratic cost function, for indoor air temperature and humidity tracking errors and sensible and latent loads. Thus, the minimization of heating and cooling demands can be also achieved. In so doing, different from classical fixed gains algorithms like PI (implemented in the previous DETECT release), the proposed approach allows one to impose, on the system under control, a dynamic behaviour that can also be optimal from the energy demand point of view. The weight matrices ( $Q$  and  $R$ , which define the cost function in eq. (11)) were set in order to impose: i) a settling time of 50 minutes for zone 1 and 10 minutes for zone 2; ii) absence of overshoots for any step variation of the reference signal. The choice of the relaxation time of zone 1 is done according to (Ghiaus C. and Hazyuk I. 2010), with the aim to ensure a smooth daily transition during the transient operation toward the regime set-point (control system is switched on from 7:00 to 18:00).

Contrarily, a faster transient requirement is imposed on the settling time of zone 2 because of its rigorous thermo hygrometric requirements. Finally, the reference input signals ( $r$  in Section 3) depends on the selected temperature and humidity set points. Note that the humidity control is obtained through the input reference set point of indoor air specific humidity ( $\omega_{sp}$ ), in order to achieve the selected relative humidity set-point ( $\phi_{sp}$ ).

## 5. Results and discussion

In the following, the results related to the effectiveness assessment of the novel DETECT control approach, in imposing reference indoor air temperature and humidity dynamics, are shown. The analysis refers to both the investigated thermal zones 1 and 2. As mentioned above, temperature and humidity are controlled daily from 07:00 to 18:00 in zone 1 and 24/7 in zone 2 (for preservation purposes of the exhibited items). Fig. 4 shows the dynamic trend of zone 1 indoor air temperature, for two sample winter days (January 13<sup>th</sup> and 14<sup>th</sup>, i.e. the 13<sup>th</sup> and 14<sup>th</sup> days of the year) and for two sample summer days (July 25<sup>th</sup> and 26<sup>th</sup>, i.e. the 206<sup>th</sup> and 207<sup>th</sup> days of the year). Here, a satisfactory performance of the developed closed-loop control scheme can be observed (coincident reference and obtained temperature profiles). Note that the set point temperature shifts from 19°C (for the winter season) to 25°C (for the cooling season). In Fig. 5 the time history of the indoor air temperature during the transient HVAC system regime (settling time from 07:00 to 08:30) is shown for January 13<sup>th</sup>. Also here the obtained temperature profile overlaps the desired reference one.

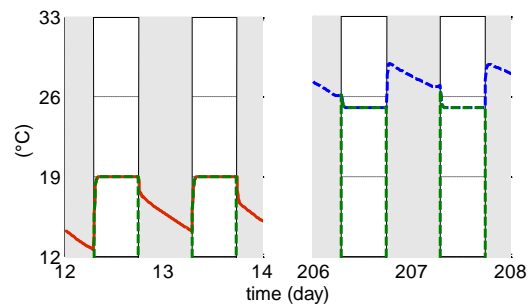


Fig. 4 – Zone 1 - Controlled indoor air temperature (red solid line for January 13<sup>th</sup> and 14<sup>th</sup> and blue dashed line for July 25<sup>th</sup> and 26<sup>th</sup>) and reference temperatures (green dashed line).

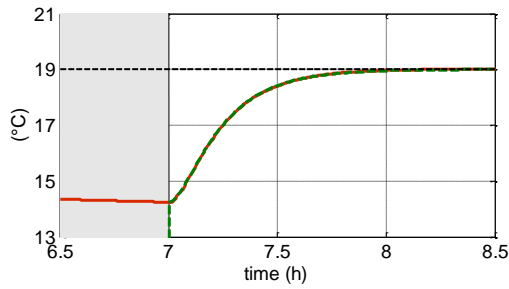


Fig. 5 – Switched on HVAC system in zone 1 in January 13th - Time history of the indoor air temperature (red solid line), reference temperature (green dashed line), set point temperature (black dashed line).

Fig. 6 shows the dynamic trend of zone 1 indoor air humidity for July 25<sup>th</sup> and 26<sup>th</sup> (Fig. 6a) and the latent load (dehumidification) resulting from the control action (Fig. 6b).

Here, the specific humidity set point is 10 g/kg, corresponding to a relative humidity of 50%. As in Fig. 5, Fig. 6c shows the time history of the indoor air humidity during the settling time, for July 26<sup>th</sup>. Note that the obtained humidity profiles overlap the desired reference ones.

In Fig. 7, the sensible thermal load ( $\dot{Q}_{AC,I}$ ), calculated according to the temperature control of Fig. 4, is reported. A similar behaviour is obtained for  $\dot{Q}_{AC,I}^{lat}$  (not shown for sake of brevity).

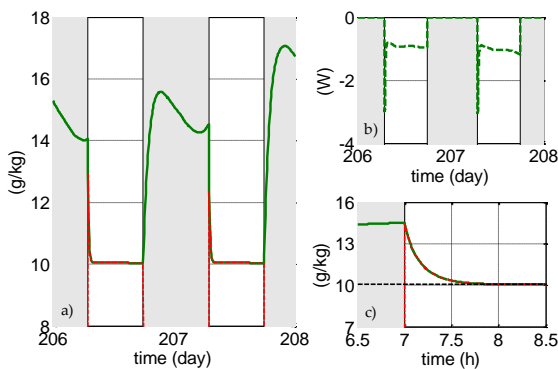


Fig. 6 – Zone 1: a) controlled indoor air humidity (green solid line), b) latent thermal load (green dashed line), c) humidity time history during the settling time (green solid line) - Reference humidity (red dashed line).

In all these figures, the grey shaded regions refer to unoccupied hours, during which the HVAC system is switched off and free floating thermo-hygrometric conditions and null control actions occur.

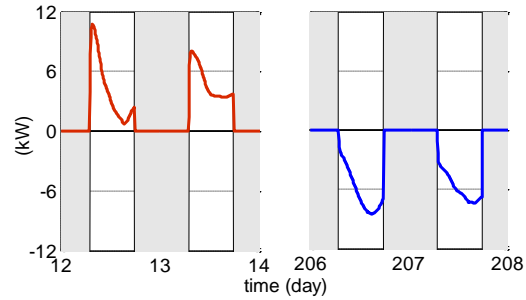


Fig. 7 – Time history of zone 1 sensible thermal load (red line heating mode - January 13<sup>th</sup> and 14<sup>th</sup>, blue line for cooling mode - July 25<sup>th</sup> and 26<sup>th</sup>) -  $\dot{Q}_{AC,I}$ .

With the help of these simulation results, some conclusions can be highlighted, such as: i) temperature and humidity set points (control aim) are always satisfactorily achieved for any initial indoor air temperature and humidity and every disturbance; ii) typical exponential behaviours of asymptotically stable liner-time-invariant systems (with unit gain, real eigenvalues and a settling time of about one hour) occur for both the temperature and humidity controls during the transient HVAC regimes; iii) smooth dynamic trends of the controlled variables and corresponding heating and cooling demands (control actions) are obtained. It is noteworthy to remark that a good tracking performance of the closed-loop controls is achieved. Very low root mean squared errors are obtained (0.024°C and 1.21·10<sup>-7</sup> g/kg for the air temperature and humidity control, respectively).

In Fig. 8, for zone 2 (where a continuous control of both the temperature and humidity is required), the obtained regulation error for the indoor air temperature is shown (from April 29<sup>th</sup> to May 2<sup>nd</sup>). Such control error is bounded within 0.01°C, despite the significant oscillation of the yearly indoor air temperature of zone 1 (which range from the minimum winter temperature of 12°C and the maximum summer one of 30°C).

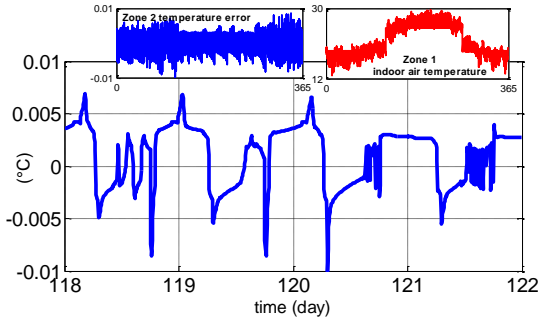


Fig. 8 – Regulation temperature error within zone 2 and indoor air temperature of zone 1 (up-right corner).

Correspondingly, the humidity control error vs. the selected set point in zone 2 is lower than  $10^{-8}$  for the entire simulated year, despite a significant zone 1 humidity variation (from 4- to 15-g/kg), as clearly depicted in Fig. 9.

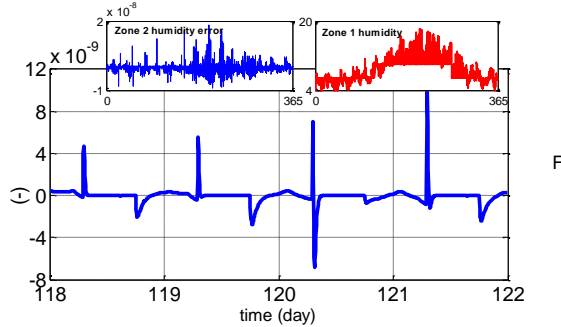


Fig. 9 – Regulation humidity error within zone 2 and indoor air humidity of zone 1 (up-right corner).

Obviously, bounded control actions are the result of bounded control gains, as clearly shown in Fig. 10. Here, as an example, the dynamic trend of the sensible thermal load of zone 2 ( $\dot{Q}_{AC,2}$ ), resulting from the control of the indoor air temperature from April 29<sup>th</sup> to May 2<sup>nd</sup> (see also Fig. 8) is reported. As expected, the zone 2 thermal loads are much smaller than those in zone 1. Note that, in Fig. 10, heating and cooling loads (as well as humidification and dehumidification demands) are detected, because of the continuous thermo-hygrometric control (i.e. no grey shaded regions occur in figure).

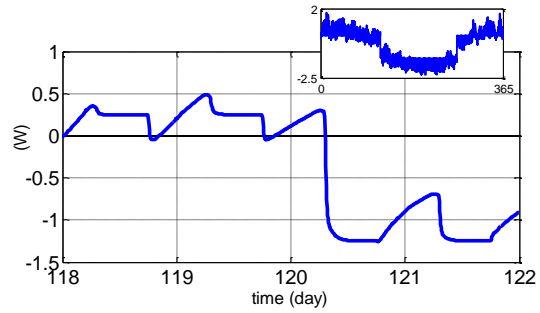


Fig. 10 – Time history of zone 2 sensible thermal load -  $\dot{Q}_{AC,2}$ .

Finally, in Fig. 11 for both the investigated thermal zones, the calculated heating and cooling (sensible and latent) yearly unitary demands, are shown. Here, it can be observed that the cooling demands are remarkably higher than the heating ones (according to the high internal gains assumed for zone 1 and to the simulated weather conditions). In addition, it is worth noting that for zone 2 the humidification and dehumidification demands vs. the sensible ones are proportionally higher than those occurring in zone 1.

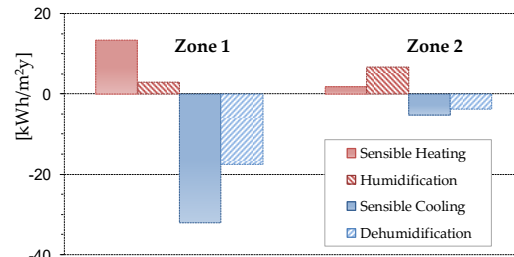


Fig. 11 – Heating and cooling sensible and latent demands.

This result is due to the continuous humidity control of zone 2 and to the considered indoor air temperature and relative humidity set points ( $T_{in,2} = 20^{\circ}\text{C}$ ,  $\phi_{sp} = 65\%$ ). Notice that, during the heating and cooling periods selected for the thermal zone 1, the humidification and dehumidification requirements of zone 2 are about 78 and 89% of the related yearly calculated demands, respectively.

## 6. Conclusion

In this paper, new features of the in-house developed computer code (called DETECT 2.3) for the building dynamic energy performance simulation are presented. The code, developed for

research purposes, enables the authors to model and analyse new prototypal technologies, non-standard operating conditions, particular system scheduling, etc., which cannot be deal with (or simultaneously taken into account) through commercial BEPS codes. From this point of view, another advantage of DETECT is the possibility to update and modify all the included models for each occurring research need. With the help of the presented code release, multi-zone buildings, consisting of thermal zones totally enclosed into others, can be modelled. In addition, all the simulated zones can be governed by rigid assigned thermo-hygrometric constraints.

This is accomplished through an innovative adaptive control strategy (called LQ-EMRAC). Here, the online adaptation of the control gains is achieved in order to assure the minimization of a quadratic cost function, which weights both the temperature / humidity tracking error and the sensible / latent energy demand. The control algorithm was designed on a simplified fourth order model. Then, it was tested and applied on the original and detailed DETECT one, based on more than 70 differential equations.

In this paper, the effectiveness of the proposed novel building simulation tool was verified through a suitable case study in which two thermal zones of a museum building are modelled. Here, a glass display case with a rigid temperature / humidity micro-climate control (for preserving aims) is enclosed in a large indoor space. Simulation results show very good tracking performance of air temperature and humidity, simultaneously, in both the simulated thermal zones. Bounded control gains and heating and cooling loads (during the transient regime) are obtained. Results also confirm the robustness of the developed control approach for unmodelled dynamics.

## Appendix

The LQ-EMRAC control action is:

$$u(t) = u_{MRAC}(t) + u_I(t) + u_E(t) \quad (13)$$

with  $u_{MRAC}(t) = K(t)x(t) + K_R(t)r(t)$ ,  $u_I(t) = K_I(t)\text{sgn}(y_e(t))$ ,

$u_I(t) = K_I(t)x_I(t)$  and  $x_I(t) = \int_{t_0}^t x_e(\tau)d\tau$ . The time-varying control gains (adaptive gains) are computed as:

$$\begin{aligned} K(t) &= \int_{t_0}^t y_e(\tau)x^T(\tau)\Gamma_\alpha d\tau + y_e(t)x^T(t)\Gamma_\beta \\ K_R(t) &= \int_{t_0}^t y_e(\tau)r(\tau)\Psi_\alpha d\tau + y_e(t)r(t)\Psi_\beta \\ K_I(t) &= \int_{t_0}^t y_e(\tau)x_I^T(\tau)\Omega_\alpha d\tau + y_e(t)x_I^T(t)\Omega_\beta \\ K_E(t) &= \gamma \int_{t_0}^t |y_e| d\tau \end{aligned} \quad (14)$$

where  $\Gamma_\alpha, \Gamma_\beta, \Omega_\alpha, \Omega_\beta \in \Lambda_n$ , with  $\Lambda_n$  being the subspace of diagonal matrices in  $\mathfrak{R}^{n \times n}$  and  $\Psi_\alpha, \Psi_\beta, \gamma \in \mathfrak{R}$  are some adaptive weights with the same sign of  $K_R^{opt}$  assumed to be known (Ioannou P. and Fidan B. 2006). The output error  $y_e$  is computed as  $y_e(t) = C_e x_e(t)$ , being  $x_e(t) = x_m(t) - x(t)$  and  $C_e = B_m^T P$  with  $P$  solution of the Lyapunov equation (Anderson B.D.O. and Moore J.B. (1971),  $PA_m + A_m^T P = -M, M > 0$ ).

## Nomenclature

### Symbols

$C$	thermal capacitance (J/K)
$h$	convective heat transfer coeff. ( $W/m^2K$ )
$h_{vs}$	water latent evaporation heat (J/g)
$I$	irradiance ( $W/m^2$ )
$\dot{m}$	flow rate (g/s)
$\dot{Q}$	thermal load (W)
$R$	thermal resistance (K/W)
$T$	temperature (K)
$t$	time (s)
$\omega$	air specific humidity (g/g)
$\Omega$	dry air mass (g)

### Subscripts/Superscripts

AC	referred to the HVAC system
cond	conduction
conv	convection
eq	equivalent
ext	external
g	internal gain
glob	global
gr	ground
in	indoor air
int	internal
lat	latent
out	outdoor air

$v$  ventilation  
 $w$  enclosed zone envelope  
 $wg$  water vapour

## References

- Anderson B.D.O. and Moore J.B. (1971). *Linear Optimal Control*, Englewood Cliff NJ, Prentice Hall.
- Buonomano A. and Palombo A. (2014). "Building energy performance analysis by an in-house developed dynamic simulation code: An investigation for different case studies." *Applied Energy* 113(0): 788-807.
- Di Bernardo M. et al. (2008). "Novel hybrid MRAC-LQ control schemes: synthesis, analysis and applications." *International Journal of Control* 81(6): 940-961.
- Ghiaus C. (2014). "Linear algebra solution to psychometric analysis of air-conditioning systems." *Energy* 74(0): 555-566.
- Ghiaus C. and Hazyuk I. (2010). "Calculation of optimal thermal load of intermittently heated buildings." *Energy and Buildings* 42(8): 1248-1258.
- Ioannou P. and Fidan B. (2006). *Adaptive Control Tutorial: Advances in Design and Control*, SIAM.
- Landau I. D. (1979). *Adaptive Control, the model reference approach*, Springer-Verlag.
- Pedro A. and Sala A. (2004). *Multivariable Control Systems: An Engineering Approach*, Springer.
- Shaikh P. H. et al. (2014). "A review on optimized control systems for building energy and comfort management of smart sustainable buildings." *Renewable and Sustainable Energy Reviews* 34(0): 409-429.